Proc. Indian Acad. Sci. (Chem. Sci.), Vol. 95, No. 3, August 1985, pp. 285–290.

Structural and catalytic studies of promoted iron oxide catalysts used in the dehydrogenation of ethylbenzene to styrene

B A SAYYED, M P GUPTA, S K DATE*, K R KAMBLE†, A Y SONSALE† and A K CHATTERJEE†

Physical Chemistry Division, National Chemical Laboratory, Pune 411 008, India
† Inorganic Chemistry Division, National Chemical Laboratory, Pune 411 008, India

MS received 13 July 1984; revised 17 December 1984

Abstract. Alkali-ion promoted iron oxide was used as a catalyst for the non-oxidative dehydrogenation of ethylbenzene to styrene. Catalytic performance studies showed high activity, with selectivity $\approx 93\%$ and conversion $\approx 49\%$. The fresh and used catalysts were characterised by various physicochemical techniques like scanning electron microscopy, x-ray diffraction and Mössbauer spectroscopy. X-ray and Mössbauer data clearly show the presence of α-Fe_2O_3 and Fe_3O_4 in the used catalysts and α-Fe_2O_3 in the fresh catalyst, the phases being identified from their standard d values and hyperfine interaction parameters.

Keywords. Promoted iron oxide catalysts; ethylbenzene dehydrogenation; Mössbauer studies.

1. Introduction

Styrene is produced commercially by the catalytic dehydrogenation of ethylbenzene in the vapour phase. This is an endothermic reaction effected by an equilibrium which favours the products as the temperature is increased and the pressure reduced. Superheated steam is used to provide heat needed for the reaction, to reduce the ethylbenzene and hydrogen partial pressures for maximising yields, and to keep the catalyst clean and active (Kaeding 1973; Sittig 1978).

Alkali promoted iron oxide is known to be distinctly better than any other catalyst with an activity over an order of magnitude higher than the unpromoted oxide and is favoured in the industrial process for ethylbenzene conversion (Lee 1973; Scheeline 1977; Courty and Le Page 1979). Although several catalytic performance studies have been carried out, there is a dearth of physicochemical characterisation studies for these catalysts leading to explanations regarding active species and catalytic performance.

In this study, we report the preparation, structural characterisation and catalytic performance of a potassia promoted, chromia stabilised iron oxide catalyst similar to the commercial catalyst Shell 105. The structural changes occurring during the catalytic conversion have been investigated by x-ray diffraction (XRD), Scanning electron microscopy (SEM) and Fe^{57} Mössbauer spectroscopy. Our results clearly indicate the formation of a spinel phase, namely Fe_3O_4 during the reaction. Other complex phases like $FeCr_2O_4$, $K_2Fe_{22}O_{34}$, etc. were not observed.

* To whom the correspondence may be addressed.

2. Experimental

2.1 *Catalyst preparation*

The α-$Fe_2O_3 + Cr_2O_3 + K_2O$ catalyst was prepared by the coprecipitation technique. Iron hydroxide was first precipitated from a solution of iron nitrate by the addition of NH_4OH. The resultant precipitate was partially dried and soluble salts of potassium carbonate and potassium dichromate were added. The slurry was washed, dried, finely ground and then transformed into 5 mm diameter pellets. The product was calcined at 700°C in air for 3 hours. Quantitative chemical analysis of the catalyst gave the following composition: Fe_2O_3 (88·4 wt %) K_2O (8·9 wt %) Cr_2O_3 (1·7 wt %).

2.2 *Catalyst characterisation and reaction procedure*

Pellets of freshly calcined and used catalysts were finely powdered and characterised by XRD, SEM and Fe^{57} Mössbauer spectroscopy. XRD patterns were recorded on a Philips PW 1730 x-ray diffractometer using CuKα-radiation with a nickel filter (λ = 1·54 Å). Scanning electron micrographs were recorded on a Cambridge stereoscan 150 microscope. Mössbauer spectra were recorded with a conventional constant acceleration electromechanical drive coupled to a nuclear data (model no. ND 100) multichannel analyser operating in the time mode. A 25 mCi ^{57}Co:Rh source was used to record the spectra at room temperature. A metallic iron foil (25 μ) was used to calibrate the spectrometer and all isomer shifts were measured with respect to that of metallic iron. Hyperfine interaction parameters were computed using an iterative, non-linear least square MOSFIT program on an ICL 1409S computer.

The continuous flow dehydrogenation reaction was carried out on a fixed bed reactor at atmospheric pressure. Five grams of the catalyst in the form of pellets were packed into the metallic reactor placed in an electrically heated tubular furnace. Temperature was maintained within an accuracy of $\pm$ 5°C by an on-off type temperature controller using a calibrated chromel-alumel thermocouple kept at the center of the catalyst bed.

Catalytic runs were carried out under fixed reaction conditions (table 1). The organic effluents were collected at regular intervals and analysed by gas chromatography. A 2 m column packed with 5 % diisodecyl phthalate and Bentone-34 was used for the analysis at 373 K.

Table 1. Catalytic performance data for the dehydrogenation reaction.

Experimental conditions:
Feed: EB : H_2O = 1 : 2·25 mole
Temperature: 883 K
*W.H.S.V. in hr^{-1}: 0·7
Conversion of EB in mole %: 49
Selectivity to styrene in mole %: 93
Product distribution in weight %:
Benzene = 1
Toluene = 1·6
Ethylbenzene (EB) = 63·6
Styrene = 34·0

*Weight hourly space velocity.

3. Results and discussion

3.1 *Catalytic activity*

The non-oxidative dehydrogenation of ethylbenzene over iron-oxide catalysts gives styrene as the major product and small amounts of benzene and toluene as by-products.

The main reaction can be expressed as:

$$C_6H_5C_2H_5 \rightleftharpoons C_6H_5CH{=}CH_2 + H_2. \tag{1}$$

Potassium carbonate and chromium oxide are incorporated into the catalyst as the promoter and the stabiliser respectively. Lee (1973) has proposed that the potassium promoter operates specifically at the surface of the catalyst and increases the catalytic activity by promoting electron transfer at the solid-gas interface. Catalytic performances under fixed experimental conditions were evaluated as follows:

Ethylbenzene (EB) conversion, C (%, mole)

$$= (\mathrm{EB}_{\mathrm{inlet}} - \mathrm{EB}_{\mathrm{outlet}}/\mathrm{EB}_{\mathrm{inlet}}) \times 100 \tag{2}$$

Product selectivity, Si (%, mole)

$$= (\text{Product } (i)/\mathrm{EB}_{\mathrm{inlet}} - \mathrm{EB}_{\mathrm{outlet}}) \times 100 \tag{3}$$

Product yield, Yi (%, mole)

$$= (\text{Product } (i)/\mathrm{EB}_{\mathrm{inlet}}) \times 100 \tag{4}$$

with yield = conversion × selectivity for a given product.

Table 1 gives the catalytic performance results of a typical run carried out for twenty hours. A high selectivity to styrene $\approx$ 93% with EB conversions $\approx$ 49% was observed. Yields of toluene were larger than benzene as observed for commercial catalysts (Wang *et al* 1983; Lee 1973). Catalytic activity was tested over an extended period $\approx$ 80 hrs. Figure 1 shows schematically the catalytic performance as a function of time on stream during two runs. The selectivity to styrene increases rapidly to 93% within the first few hours and remains steady with time on stream for both runs.

Percentage yields of side products toluene and benzene were low 1–2%. Lower yields of toluene and benzene during the first run are attributed to the increased coking rate caused by the increased EB feed. Coking decreases the acidic centres and dealkylation which takes place at Bronsted acid centres also decreases (Kulkarni and Kulkarni 1983).

Since the selectivity to styrene was found to be very high in these catalytic runs, physicochemical characterisation of these catalysts was undertaken using various techniques like XRD, SEM and Fe^{57} Mössbauer spectroscopy. These techniques have provided valuable information about the crystallite sizes and distribution of different phases formed during conversion.

3.2 *X-ray diffraction studies*

From a systematic analysis of the d values of the observed x-ray peaks with the help of standard ASTM data, it is possible to identify the pattern as due to the single phase of α-Fe_2O_3 in fresh catalyst.

Crystallite sizes were calculated from x-ray line broadening using the Scherrer equation

$$D = K\lambda/\beta \cos\theta,$$

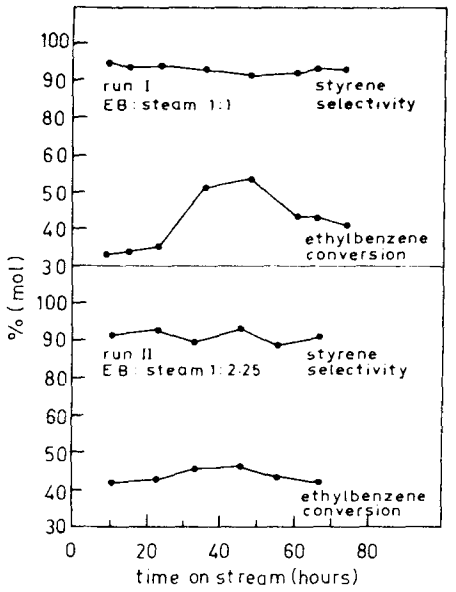

Figure 1. Selectivity to styrene and ethylbenzene conversion over iron oxide catalysts for run I (EB to steam ratio = 1 : 1) and run II (EB to steam ratio = 1 : 2·25) with time on stream.

where λ = 1·543 Å, θ is the Bragg angle and β the pure diffraction broadening (Klug and Alexander 1974). The fresh catalyst showed a distribution of crystallite sizes, 355 Å, 883 Å and 1025 Å, determined from the major reflections (104), (024) and (110) of the α-Fe_2O_3 structure.

An x-ray diffractogram of the used catalyst was analysed in a similar fashion. From a comparison with ASTM data it was easy to assign patterns to Fe_3O_4 and K_2CrO_4 as major phases. Traces of α-Fe_2O_3 are also present. The lattice parameter for Fe_3O_4 (a_0 = 8·38 Å) was close to that of bulk magnetite (a_0 = 8·376 Å. The average crystallite size from x-ray line broadening was 378 Å determined from the intense (220), (311) and (400) reflections of the Fe_3O_4 structure. Crystallite sizes were found to be more uniform after the catalytic dehydrogenation reaction.

The XRD patterns did not show the presence of $FeCr_2O_4$ and $K_2Fe_{22}O_{34}$ phases, previously observed in iron oxide catalysts (Shibata and Kiyoura 1969; Courty and Marcilly 1983). However, minute quantities of these compounds may be present below the XRD detection limit.

SEM photographs of the fresh and used catalyst pellets showed the presence of large particles with sizes ranging from 5000–20,000 Å. The fresh catalyst had well-defined particles. In the used catalyst, small clusters were deposited on the large particles and their formation may be attributed to reduction of the catalyst. Particle sizes for the fresh and used catalyst do not change. Courty and LePage (1979) have attributed increased selectivity for dehydrogenation of ethylbenzene to large particle sizes ($\approx$ 5000 Å).

3.3 *Fe^{57} Mössbauer spectroscopic analysis*

Least squares fitting and an analysis of the six line hyperfine split Mössbauer spectrum gave hyperfine interaction parameters as shown in table 2. From a comparison with

Table 2. Hyperfine interaction parameters derived from room temperature Mössbauer spectra for fresh and used catalysts.

Mössbauer parameters	Fresh catalyst α-Fe_2O_3	Used catalyst		
		α-Fe_2O_3	$Fe_3O_4{}^A$	$Fe_3O_4{}^B$
I.S. ($\pm$0·02 mm/sec)	0·43	0·31	0·29	0·69
ΔE_Q ($\pm$0·05 mm/sec)	0·20	0·15	−0·01	0·05
H_n/KO_e ($\pm$5 KO_e)	515	510	497	459
Line width ($\pm$0·05 mm/sec)	0·39	0·60	0·60	0·73

I.S. ≡ Isomer or chemical shift (δ); ΔE_Q ≡ Quadrupole splitting; H_n ≡ Hyperfine field in Kilo oersteds (KOe). ^{A,B}Tetrahedral or Octahedral sites.

literature values, the six line pattern was assigned to Fe^{3+} ions in α-Fe_2O_3 (Greenwood and Gibb 1971). This result agrees well with the XRD data.

After a careful analysis of the broad experimental spectrum of the used catalyst after 80 hours of dehydrogenation, three sextets were resolved. The derived hyperfine parameters given in table 2 are characteristic of Fe^{3+} in α-Fe_2O_3, Fe^{3+} (A) and Fe^{3+}/Fe^{2+} (B) in Fe_3O_4 (MEDI 1974). The parameters show an excellent agreement with corresponding values reported in the literature for pure phases (Kundig and Hargrove 1969). The ratio of α-Fe_2O_3: Fe_3O_4 was found to be 0·03, indicating that a large amount of α-Fe_2O_3 was reduced to Fe_3O_4 during the reaction. Because of the high sensitivity and resolution of the Mössbauer spectroscopic technique, it was possible to identify the α-Fe_2O_3 phase even in the presence of a large amount of Fe_3O_4. However no interaction of the promoter (K_2O) and stabiliser (Cr_2O_3) with the main active agent α-Fe_2O_3 was observed. The fresh and used catalysts have been studied by conversion electron Mössbauer spectroscopy to identify additional species, if any, present on the surface. In addition to the bulk species, namely α-Fe_2O_3 (fresh catalyst) and α-Fe_2O_3, Fe_3O_4 (used catalyst), a small concentration of new surface species α-FeOOH (used catalyst) have been identified through their characteristic hyperfine interaction parameters (δ = 0·321 mm/sec, ΔE_Q = 0·036 mm/sec, H_n = 376 KO_e) (Tricker *et al* 1982).

From the characterisation studies using bulk techniques, partial reduction of α-Fe_2O_3 to Fe_3O_4, but no subsequent reduction to metallic iron, was observed. The rate of reduction to Fe_3O_4 is lowered by steam (Viswanath *et al* 1975). Because of the simultaneous presence of hydrogen and steam a steady state is established between the two phases.

$$\alpha\text{-}Fe_2O_3 \underset{H_2O}{\overset{H_2}{\rightleftharpoons}} Fe_3O_4$$

Since the reduction of α-Fe_2O_3 to Fe_3O_4 is rapid, the steady state (composed of a mixture of Fe_2O_3/Fe_3O_4) is attained after a few hours under operating conditions. The active interface, with a distribution of acidic-basic sites is one of the factors responsible for high activity/selectivity of the catalyst (Ai 1979; Murakami *et al* 1981; Tagawa *et al* 1982). The reduction of α-Fe_2O_3 to metallic iron is avoided because of the high

P_{H_2O}/P_{H_2} value and the large amount of lattice disorder (Pernicone and Traina 1979). Distribution of Cr^{3+} in the catalyst also delays the α-Fe_2O_3 reduction (Kung *et al* 1981). However chromia concentration in the catalyst is too low to have a significant effect.

4. Conclusion

In summary, it is seen that the α-Fe_2O_3-Cr_2O_3-K_2O catalyst has exhibited very high activity/selectivity over an extended period of time. Physicochemical characterisation has identified the changes occuring during the catalytic reaction *i.e.* the partial reduction of α-Fe_2O_3 to Fe_3O_4 and stabilisation of these two phases in the bulk.

Acknowledgements

The authors thank Dr P Ratnasamy and Dr A P B Sinha for many useful discussions and INSA, New Delhi for partial support. One of us (BS) thanks INSA for a fellowship.

References

Ai M 1979 *J. Catal.* **60** 306
Courty Ph and Le Page J F 1979 in *Preparation of catalysts II* (eds) B Delmon, P A Jacobs and G Poncelet (Amsterdam: Elsevier) p. 293 and references therein
Courty Ph and Marcilly Ch 1983 in *Preparation of catalysts III* (eds) G Poncelet, P Grange and P A Jacobs (Amsterdam: Elsevier) p. 509
Greenwood N N and Gibb T C 1971 in *Mössbauer spectroscopy* (London: Chapman and Hall) p. 240
Kaeding W W 1973 *Catal. Rev.* **8** 307
Klug H P and Alexander L E 1974 in *X-ray diffraction procedures* 2nd ed. (New York: Wiley) p. 491
Kulkarni S J and Kulkarni S B 1983 in *React. Kinet. Catal. Lett.* **22** 29
Kundig W and Hargrove R S 1969 *Solid State Commun.* **7** 223
Kung H H, Kung M C and Yang B L 1981 *J. Catal.* **69** 506
Lee E H 1973 *Catal. Rev.* **8** 285
MEDI 1974 *Mössbauer effect data index* (eds) J G Stevens and V E Stevens (New York: Plenum Press) p. 85
Murakami Y, Iwayama K, Uchida H, Hattori T and Tagawa T 1981 *J. Catal.* **71** 257
Pernicone N and Traina F 1979 in *Preparation of catalysts II* (eds) B Delmon, P A Jacobs and G Poncelet (Amsterdam: Elsevier) p. 334
Scheeline H W 1977 SRI Report No. 33B, 73, 87
Shibata K and Kiyoura T 1969 *J. Catal.* **13** 103
Sittig M 1978 in *Handbook of catalyst manufacture* (New Jersey: Noyes Data Corp.) p. 240
Tagawa T, Hattori T and Murakami Y 1982 *J. Catal.* **75** 66
Tricker M J, Vaishnava P P and Whan D A 1982 *Appl. Catal.* **3** 283
Viswanath R P, Viswanathan B and Sastri M V C 1975 *React. Kinet. Catal. Lett.* **2** 51
Wang I, Chang W F, Shiau R J, Wu J C and Chung C S 1983 *J. Catal.* **83** 428